

# Consistent description of $^{12}\text{C}$ and $^{16}\text{O}$ using finite range three-body interaction

N. Itagaki

*Yukawa Institute for Theoretical Physics, Kyoto University,  
Kitashirakawa Oiwake-Cho, Kyoto 606-8502, Japan*

(Dated: March 21, 2022)

Consistent description of  $^{12}\text{C}$  and  $^{16}\text{O}$  has been a long standing problem of microscopic  $\alpha$  cluster models, where the wave function is fully antisymmetrized and the effective interaction is applied not between  $\alpha$  clusters but between nucleons. When the effective interaction is designed to reproduce the binding energy of  $^{16}\text{O}$  (four  $\alpha$ ), the binding energy of  $^{12}\text{C}$  (three  $\alpha$ ) becomes underbound by about 10 MeV. In the present study, by taking into account the coupling with the  $jj$ -coupling shell model components and utilizing Tohsaki interaction, which is phenomenological but has finite-range three-body interaction terms, we show that consistent understanding of these nuclei can be achieved. The original Tohsaki interaction gives small overbound of about 3 MeV for  $^{16}\text{O}$ , and this is improved by slightly modifying three-body Majorana exchange parameter. Also, the coupling with the  $jj$ -coupling shell model wave function strongly contributes to the increase of the binding energy of  $^{12}\text{C}$ . So far the application of Tohsaki interaction has been limited to  $4N$  nuclei, and here, we add Bartlett and Heisenberg exchange terms in the two-body interaction for the purpose of applying it to neutron-rich systems, and it is applied to  $^6\text{He}$ .

PACS numbers: 21.30.Fe, 21.60.Cs, 21.60.Gx, 27.20.+n

## I. INTRODUCTION

The nuclei  $^{12}\text{C}$  and  $^{16}\text{O}$  are typical light nuclei, and they have been extensively studied based on the cluster approaches [1]. Since there is no bound nucleus with mass number 5 or 8, formation of  $^{12}\text{C}$  from three  $^4\text{He}$  nuclei ( $\alpha$  clusters) is a key process of the nucleosynthesis. Here, the second  $0^+$  state at  $E_x = 7.6542$  MeV plays a crucial role, which is the second excited state of  $^{12}\text{C}$  and located just above the threshold energy to decay into three  $^4\text{He}$  nuclei [2]. The existence of three  $\alpha$  state just at this energy is essential factor in the synthesis of various elements in stars. For also  $^{16}\text{O}$ , cluster structure has been shown to be extremely important. Although the ground state corresponds to the doubly closed  $p$  shell of the shell model, this configuration can be also interpreted from four  $\alpha$  and  $^{12}\text{C}+\alpha$  view points, if we take certain limit for the inter cluster distances. Also the first excited state of  $^{16}\text{O}$  at  $E_x = 6.0494$  MeV, very close to the threshold to decay into  $^{12}\text{C}$  and  $^4\text{He}$ , can be interpreted as  $^{12}\text{C}+^4\text{He}$  cluster state [3], and low-lying cluster states just around the threshold are quite important in the synthesis of  $^{16}\text{O}$  in stars [4]. Various cluster models have been proposed and successfully applied to these nuclei.

However consistent description of  $^{12}\text{C}$  and  $^{16}\text{O}$  has been a long standing problem of microscopic  $\alpha$  cluster models. Here the definition of the microscopic model is that the wave function is fully antisymmetrized and the effective interaction is applied not between  $\alpha$  clusters but between nucleons. When the effective interaction is designed to reproduce the binding energy of  $^{16}\text{O}$  (four  $\alpha$ ), the binding energy of  $^{12}\text{C}$  (three  $\alpha$ ) becomes underbound by about 10 MeV, and on the contrary, when the binding energy of  $^{12}\text{C}$  is reproduced,  $^{16}\text{O}$  becomes overbound by about 20 MeV. We have previously utilized Tohsaki interaction [5], which has finite-range three-body terms,

and the obtained result is better than ones only within the two-body terms; however the problem has not been fully solved [6].

One of the clue to solve this problem is the inclusion of the spin-orbit interaction. In most of the cluster models,  $\alpha$  clusters are defined as simple  $(0s)^4$  configuration at some point. These  $\alpha$  clusters are spin singlet systems and the spin-orbit interaction does not contribute inside  $\alpha$  clusters and also between  $\alpha$  clusters. In  $jj$ -coupling shell model, the spin-orbit interaction is quite important and this plays an essential role in explaining the observed magic numbers. According to the  $jj$ -coupling shell model,  $^{12}\text{C}$  corresponds to the subclosure configuration of spin-orbit attractive orbits ( $p_{3/2}$ ) and the spin-orbit interaction works attractively, whereas  $^{16}\text{O}$  corresponds to the closure of major shell ( $p$  shell), where both spin-orbit attractive ( $p_{3/2}$ ) and repulsive ( $p_{1/2}$ ) orbits are filled and the contribution of the spin-orbit interaction cancels. Therefore, inclusion of the  $\alpha$  breaking wave function and taking into account the spin-orbit contribution are expected to decrease the binding energy difference of  $^{12}\text{C}$  and  $^{16}\text{O}$ . To describe the  $jj$ -coupling shell model states with the spin-orbit contribution starting with the cluster model wave function, we proposed the antisymmetrized quasi-cluster model (AQCM) [7–13]. In the AQCM, the transition from the cluster- to shell-model-structure can be described by only two parameters:  $R$  representing the distance between  $\alpha$  clusters and  $\Lambda$ , which characterizes the transition of  $\alpha$  cluster(s) to quasi-cluster(s) and quantifies the role of the spin-orbit interaction.

In nuclear structure calculations, it is quite well known that the central part of the nucleon-nucleon interaction in the calculation should have proper density dependence in order to satisfy the saturation property of nuclear systems. If we just introduce simple two-body interaction, for instance Volkov interaction [14], which has been

widely used in the cluster studies, we have to properly choose Majorana exchange parameter for each nucleus, and consistent description of two different nuclei with the same Hamiltonian becomes a tough work. Thus it is rather difficult to reproduce the threshold energies to decay into different subsystems.

Concerning the density dependence of the interaction, adding zero range three-body interaction term helps better agreements with experiments as in modified Volkov (MV) interaction [15]. However, in this case the binding energies become quite sensitive to the choice of the size parameter of Gaussian-type single particle wave function. Especially, the binding energy and radius of  ${}^4\text{He}$  cannot be reproduced consistently. This situation is essentially common in the case of Gogny interaction widely used in mean field studies [16]. The nucleus  ${}^4\text{He}$  is a building block of  $\alpha$  cluster states and it is desired that the size and binding energy are reproduced. The Tohsaki interaction, which has finite range three-body terms, has much advantages compared with the zero range three-body interactions. This interaction is a phenomenological one and designed to reproduce the  $\alpha$ - $\alpha$  scattering phase shift. Also it gives reasonable size and binding energy of the  $\alpha$  cluster, which is rather difficult in the case of zero-range three-body interaction, and the binding energy is less sensitive to the choice of size parameter of Gaussian-type single particle wave function because of the finite range effect of the three-body interaction. Furthermore, the saturation properties of nuclear matter is reproduced rather satisfactory.

Of course, introducing the term proportional to the fractional power of the density is another possibility to reproduce the saturation properties of nuclear systems as in density functional theories (DFT), instead of introducing three-body interaction terms. However, here we perform parity and angular momentum projections, and we also superpose many Slater determinants based on the generator coordinate method (GCM). In this case, it is desired that the Hamiltonian is expressed in a operator form such as three-body interaction, which enables us to calculate the transition matrix elements between different Slater determinants. From this view point, simplified version of finite range three-body interaction is proposed in Ref. [17].

The purpose of the present work is to combine the use of finite range three-body interaction for the interaction part and AQCM for the wave function part to establish consistent understanding of  ${}^{12}\text{C}$  and  ${}^{16}\text{O}$ . The original Tohsaki interaction gives small overbound for  ${}^{16}\text{O}$  (about 3 MeV) [6], and here, we try to improve by slightly modifying three-body Majorana exchange parameter. For  ${}^{12}\text{C}$ , subclosure configuration of  $jj$ -coupling shell model, where the spin-orbit interaction plays an important role, is coupled to three  $\alpha$  model spaced based on AQCM. For  ${}^{16}\text{O}$ , the closed shell configuration of the  $p$  shell is the dominant configuration of the ground state, and we apply four  $\alpha$  model, which covers the model space of closed  $p$  shell. Also, the application of Tohsaki interac-

tion has been limited to  $4N$  nuclei, and we add Bartlett and Heisenberg exchange terms in the two-body interaction for the purpose of applying it to neutron-rich systems.

## II. THE MODEL

### A. Hamiltonian

The Hamiltonian ( $\hat{H}$ ) consists of kinetic energy ( $\hat{T}$ ) and potential energy ( $\hat{V}$ ) terms,

$$\hat{H} = \hat{T} + \hat{V}, \quad (1)$$

and the kinetic energy term is described as one-body operator,

$$\hat{T} = \sum_i \hat{t}_i - T_{cm}, \quad (2)$$

and the center of mass kinetic energy ( $T_{cm}$ ), which is constant, is subtracted. The potential energy has central ( $\hat{V}_{central}$ ), spin-orbit ( $\hat{V}_{spin-orbit}$ ), and the Coulomb parts.

### B. Tohsaki Interaction

For the central part of the potential energy ( $\hat{V}_{central}$ ), we adopt Tohsaki interaction. The Tohsaki interaction consists of two-body ( $V^{(2)}$ ) and three-body ( $V^{(3)}$ ) terms:

$$\hat{V}_{central} = \frac{1}{2} \sum_{ij} V_{ij}^{(2)} + \frac{1}{6} \sum_{ijk} V_{ijk}^{(3)}, \quad (3)$$

where  $V_{ij}^{(2)}$  and  $V_{ijk}^{(3)}$  consist of three terms,

$$V_{ij}^{(2)} = \sum_{\alpha=1}^3 V_{\alpha}^{(2)} \exp[-(\vec{r}_i - \vec{r}_j)^2 / \mu_{\alpha}^2] (W_{\alpha}^{(2)} + M_{\alpha}^{(2)} P^r)_{ij}, \quad (4)$$

$$V_{ijk}^{(3)} = \sum_{\alpha=1}^3 V_{\alpha}^{(3)} \exp[-(\vec{r}_i - \vec{r}_j)^2 / \mu_{\alpha}^2 - (\vec{r}_i - \vec{r}_k)^2 / \mu_{\alpha}^2] \times (W_{\alpha}^{(3)} + M_{\alpha}^{(3)} P^r)_{ij} (W_{\alpha}^{(3)} + M_{\alpha}^{(3)} P^r)_{ik}. \quad (5)$$

Here,  $P^r$  represents the exchange of spatial part of the wave functions of interacting two nucleons, and this is equal to  $-P^{\sigma} P^{\tau}$  due to the Pauli principle ( $P^r P^{\sigma} P^{\tau} = -1$ ), where  $P^{\sigma}$  and  $P^{\tau}$  are spin and isospin exchange operators, respectively. The range parameters  $\{\mu_{\alpha}\}$  are set to be common for the two-body and three-body parts, and the values are listed in Table I together with strengths of two-body interaction  $\{V_{\alpha}^{(2)}\}$ , three-body interaction  $\{V_{\alpha}^{(3)}\}$ , and the Majorana exchange parameters

TABLE I: Parameter set for the two-body part of the Tohsaki interaction (F1 parameterization in Ref. [5]) together with the strengths of the three-body interaction.

$\alpha$	$\mu_\alpha$ (fm)	$V_\alpha^{(2)}$ (MeV)	$V_\alpha^{(3)}$ (MeV)	$M_\alpha^{(2)}$	$W_\alpha^{(2)}$
1	2.5	-5.00	-0.31	0.75	0.25
2	1.8	-43.51	7.73	0.462	0.538
3	0.7	60.38	219.0	0.522	0.478

TABLE II: Majorana exchange parameters for the three-body interaction terms. F1 stands for the original F1 set of Tohsaki interaction [5], and F1' is the modified versions introduced in the present article.

	F1	F1'
$M_1^{(3)}$	0.0	0.0
$M_2^{(3)}$	0.0	0.0
$M_3^{(3)}$	1.909	1.5

of the two-body interaction. The values of Wigner parameters,  $\{W_\alpha^{(2)}\}$ , are given as  $W_\alpha^{(2)} = 1 - M_\alpha^{(2)}$ . We employ F1 parameter set in Ref. [5].

Until now Tohsaki interaction has been applied only to  $4N$  nuclei, and in this article we extend the application to neutron-rich nuclei. The original Tohsaki interaction does have Wigner and Majorana exchange terms, but spin and isospin exchange terms are missing. Because of this, the interaction gives a weak bound state for a two neutron system, as in the case of Volkov interaction. Therefore, here we add Bartlett ( $BP^\sigma$ ) and Heisenberg ( $HP^\tau$ ) exchange terms in Eq. 4 as  $(W_\alpha^{(2)} + BP^\sigma - HP^\tau + M_\alpha^{(2)}P^r)_{ij}$ . The values of  $B$  and  $H$  are chosen to be 0.1. By adding these terms, the neutron-neutron interaction (or proton-proton interaction) because weaker than the original interaction, while  $\alpha$ - $\alpha$  scattering phase shift is not influenced by this modification.

### C. Spin-orbit interaction

For the spin-orbit part, G3RS [18], which is a realistic interaction originally determined to reproduce the nucleon-nucleon scattering phase shift, is adopted;

$$\hat{V}_{spin-orbit} = \frac{1}{2} \sum_{ij} V_{ij}^{ls} \quad (6)$$

$$V_{ij}^{ls} = V_{ls}(e^{-d_1(\vec{r}_i - \vec{r}_j)^2} - e^{-d_2(\vec{r}_i - \vec{r}_j)^2})P(^3O)\vec{L} \cdot \vec{S}, \quad (7)$$

where  $d_1 = 5.0 \text{ fm}^{-2}$ ,  $d_2 = 2.778 \text{ fm}^{-2}$ , and  $P(^3O)$  is a projection operator onto a triplet odd state. The operator  $\vec{L}$  stands for the relative angular momentum and  $\vec{S}$  is the total spin, ( $\vec{S} = \vec{S}_1 + \vec{S}_2$ ). The strength,  $V_{ls}$ , has been determined to reproduce the  $^4\text{He}+n$  scattering phase shift [19], and  $V_{ls} = 1600 - 2000 \text{ MeV}$  has been suggested.

### D. Single particle wave function (Brink model)

In conventional  $\alpha$  cluster models, the single particle wave function has a Gaussian shape [20];

$$\phi_i = \left(\frac{2\nu}{\pi}\right)^{\frac{3}{4}} \exp\left[-\nu(\mathbf{r}_i - \mathbf{R}_i)^2\right] \eta_i, \quad (8)$$

where  $\eta_i$  represents the spin-isospin part of the wave function, and  $\mathbf{R}_i$  is a real parameter representing the center of a Gaussian wave function for the  $i$ -th particle. In this Brink-Bloch wave function, four nucleons in one  $\alpha$  cluster share the common  $\mathbf{R}_i$  value. Hence, the contribution of the spin-orbit interaction vanishes.

### E. Single particle wave function in the AQCM

In the AQCM,  $\alpha$  clusters are changed into quasi clusters. For nucleons in the quasi cluster, the single particle wave function is described by a Gaussian wave packet, and the center of this packet  $\zeta_i$  is a complex parameter;

$$\psi_i = \left(\frac{2\nu}{\pi}\right)^{\frac{3}{4}} \exp\left[-\nu(\mathbf{r}_i - \zeta_i)^2\right] \chi_i \tau_i, \quad (9)$$

where  $\chi_i$  and  $\tau_i$  in Eq. (9) represent the spin and isospin parts of the  $i$ -th single particle wave function, respectively. The spin orientation is governed by the parameters  $\xi_{i\uparrow}$  and  $\xi_{i\downarrow}$ , which are in general complex, while the isospin part is fixed to be 'up' (proton) or 'down' (neutron),

$$\chi_i = \xi_{i\uparrow}|\uparrow\rangle + \xi_{i\downarrow}|\downarrow\rangle, \tau_i = |p\rangle \text{ or } |n\rangle. \quad (10)$$

The center of Gaussian wave packet is give as

$$\zeta_i = \mathbf{R}_i + i\Lambda e_i^{\text{spin}} \times \mathbf{R}_i, \quad (11)$$

where  $e_i^{\text{spin}}$  is a unit vector for the intrinsic-spin orientation, and  $\Lambda$  is a real control parameter describing the dissolution of the  $\alpha$  cluster. As one can see immediately, the  $\Lambda = 0$  AQCM wave function, which has no imaginary part, is the same as the conventional Brink-Bloch wave function. The AQCM wave function corresponds to the  $jj$ -coupling shell model wave function, such as subshell closure configuration, when  $\Lambda = 1$  and  $\mathbf{R}_i \rightarrow 0$ . The mathematical explanation for this is summarized in Ref. [11]. For the width parameter, we use the value of  $\nu = 0.23 \text{ fm}^{-2}$ .

### F. AQCM wave function of the total system

The wave function of the total system  $\Psi$  is antisymmetrized product of these single particle wave functions;

$$\Psi = \mathcal{A}\{\psi_1\psi_2\psi_3 \cdots \psi_A\}. \quad (12)$$

The projections onto parity and angular momentum eigen states can be performed by introducing the projection operators  $P_{MK}^J$  and  $P^\pi$ , and these are performed numerically in the actual calculation.

### G. Superposition of different configurations

Based on GCM, the superposition of different AQCM wave functions can be done,

$$\Phi = \sum_i c_i P_{MK}^J P^\pi \Psi_i. \quad (13)$$

Here,  $\{\Psi_i\}$  is a set of AQCM wave functions with different values of the  $R$  and  $\Lambda$  parameters, and the coefficients for the linear combination,  $\{c_i\}$  are obtained by solving the Hill-Wheeler equation [20]. We obtain a set of coefficients for the linear combination  $\{c_j\}$  for each eigen value of  $E$ .

## III. RESULTS

We start the application of Tohsaki interaction with  ${}^6\text{He}$ . So far Tohsaki interaction has been applied to  $4N$  nuclei, and here a neutron-rich system is examined. Figure 1 shows the energy convergence of the ground  $0^+$  state of  ${}^6\text{He}$ . The model space is  $\alpha+n+n$  and the positions of two neutrons are randomly generated, and we superpose different configurations for the neutrons. The horizontal line at  $-27.31$  MeV shows the threshold energy of  ${}^4\text{He}+n+n$  (the experimental value is  $-28.29566$  MeV). Here, the dotted line is the result of original F1 parameter set. We add the Bartlet and Heisenberg terms with the parameters of  $B = H = 0.1$ , and the result is shown as the dashed line. Furthermore, we slightly modify the Majorana exchange parameter of the three-body interaction term and the results of F1' parameter set is shown as solid line (this is to reproduce the binding energy of  ${}^{16}\text{O}$ , which will be discussed shortly). For the spin-orbit part, the strength  $V_{ls}$  has been determined to be  $1600 - 2000$  MeV in the analysis of  ${}^4\text{He}+n$  scattering phase shift [19], and here we adopted  $V_{ls} = 1600$  MeV. The results of dashed and solid lines are similar and difficult to distinguish. Nevertheless, by adding Bartlet and Heisenberg terms, we obtained the binding energy close to the experimental one (the experimental value of  $S_{2n}$  is  $0.975$  MeV).

For  ${}^{16}\text{O}$ , according to the  $jj$ -coupling shell model, the ground state corresponds to the closure of major shell ( $p$  shell), where both spin-orbit attractive ( $p_{3/2}$ ) and repulsive ( $p_{1/2}$ ) orbits are filled and the contribution of the spin-orbit interaction cancels. Therefore,  $\alpha$  breaking configurations are not expected to mix strongly, and here we introduce a four  $\alpha$  model space, which is known to coincide with the closed  $p$  shell configuration at the limit of relative distance between  $\alpha$  clusters equal to zero. The

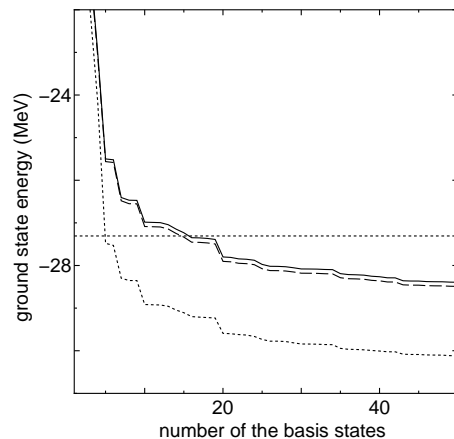


FIG. 1: The energy convergence of the ground  $0^+$  state of  ${}^6\text{He}$  with an  $\alpha+n+n$  model. We prepare different configurations for the two neutrons outside  ${}^4\text{He}$  and superpose them. The horizontal line at  $-27.31$  MeV shows the threshold energy of  ${}^4\text{He}+n+n$ . The dotted line is the result of original F1 parameter set, and the dashed line is the result after adding  $B = H = 0.1$ . The results of F1' parameter sets is shown as the solid line.

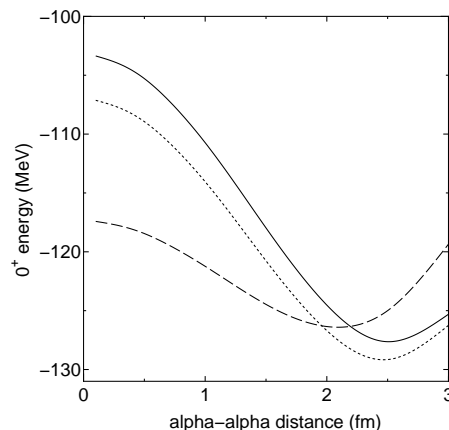


FIG. 2: The  $0^+$  energy of  ${}^{16}\text{O}$  with a tetrahedron configuration of four  $\alpha$ 's as a distance between  $\alpha$  clusters. The dotted line is the result of original F1 parameter set. The results of F1' parameter set is shown as solid line. The dashed line is for the result calculated using Volkov No.2 interaction [14] with  $M = 0.63$ .

$0^+$  energy of  ${}^{16}\text{O}$  with a tetrahedron configuration of four  $\alpha$ 's is shown in Fig. 2 as a function of the relative distance between  $\alpha$  clusters. The dotted line is the result of original F1 parameter set, and the result of newly introduced F1' parameter set is shown as the solid line. Here, F1' is designed to avoid small overbinding of  ${}^{16}\text{O}$  when the original F1 parameter set is introduced, and the solid line is less attractive compared with the dotted line by about  $2 \sim 3$  MeV. The energies of  ${}^{16}\text{O}$  is obtained by superposing the basis states with  $\alpha$ - $\alpha$  distances of 0.1, 0.5, 1.0, 1.5, 2.0, 2.5, and 3.0 fm based on GCM, and the newly introduced parameter F1' parameter set gives



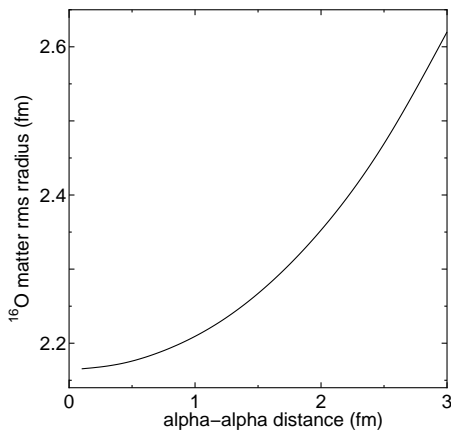


FIG. 3: . The matter rms radius for the  $0^+$  state of  $^{16}\text{O}$  calculated with the tetrahedron configuration of four  $\alpha$ 's. The horizontal axis shows the relative distance between  $\alpha$  clusters.

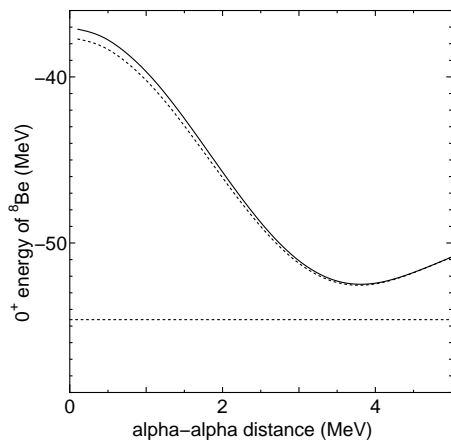


FIG. 4: The  $0^+$  energy curves of  $^8\text{Be}$  calculated with  $\alpha+\alpha$  model as a function of relative  $\alpha$ - $\alpha$  distance. The dotted and solid lines are the results calculated with the original F1 parameter set and newly introduced F1' parameter set. The dotted line at  $-54.61$  MeV shows the threshold energy of  $\alpha+\alpha$ .

$-126.9$  MeV for the ground state compared to the experimental value of  $-127.619293$  MeV.

The observed root mean square (rms) radius of  $^{16}\text{O}$  is quite large; the charge radius is  $2.69$  fm [21], and we often underestimate the radius by  $0.1$ - $0.2$  fm, if we calculate with four  $\alpha$  models and use only two-body effective interaction such as Volkov interaction [14]. The dashed line in Fig. 2 is for the result calculated using Volkov No.2 interaction with  $M = 0.63$ . In this case, the energy curve is much shallower and feature of the curve is quite different from the Tohsaki interaction cases. The dashed line shows the energy minimum point around the  $\alpha$ - $\alpha$  distance of  $2$  fm. Using the Tohsaki interaction with finite-range three-body interaction terms, the solid line in Fig. 2 shows that the lowest energy is obtained with the  $\alpha$ - $\alpha$  distance of  $2.5$  fm, larger than the result of Volkov

interaction (dashed line) by  $0.5$  fm. The matter rms radius for the  $0^+$  state of  $^{16}\text{O}$  with a tetrahedron configuration of four  $\alpha$ 's is shown in Fig. 3 as a function of distances between  $\alpha$  clusters. When the  $\alpha$ - $\alpha$  distance is  $2.5$  fm, which gives the lowest energy in the Tohsaki interaction cases, the matter radius is  $2.49$  fm. This matter radius decreases to  $2.35$  fm if the  $\alpha$ - $\alpha$  distance is  $2.0$  fm, which gives the lowest energy in the Volkov interaction case. The ground state of  $^{16}\text{O}$  obtained by superposing the basis states with the  $\alpha$ - $\alpha$  distances of  $0.1$ ,  $0.5$ ,  $1.0$ ,  $1.5$ ,  $2.0$ ,  $2.5$ , and  $3.0$  fm gives the rms matter radius of  $2.49$  fm (Tohsaki interaction F1' parameter set). This value corresponds to the charge radius of  $2.64$  fm, and the experimental value is almost reproduced.

Here we compare the F1 (original) and F1' (modified) parameter sets of the Tohsaki interaction. The  $0^+$  energy curves of  $\alpha$ - $\alpha$  ( $^8\text{Be}$ ) calculated with F1 (dotted line) and F1' (solid line) are compared in Fig. 4. As explained previously, F1' is designed to avoid small overbinding of  $^{16}\text{O}$  calculated with F1, and the solid line is slightly more repulsive at short  $\alpha$ - $\alpha$  relative distances. However the difference is quite small and less than  $1$  MeV, and the character of the original F1 that the  $\alpha$ - $\alpha$  scattering phase shift is reproduced is not influenced by this modification.

For  $^{12}\text{C}$ , we prepare  $jj$ -coupling ( $\alpha$  breaking) components of the wave functions based on AQCM. We introduce basis states with equilateral triangular configuration of three  $\alpha$  clusters with the relative distances of  $R = 0.5$ ,  $1.0$ ,  $1.5$ ,  $2.0$ ,  $2.5$ , and  $3.0$  fm and change  $\alpha$  clusters to quasi clusters by giving dissolution parameter  $\Lambda$ . The values of  $\Lambda$  are chosen to be  $0.2$  and  $0.4$ , since the states in between pure three  $\alpha$  clusters ( $\Lambda = 0$ ) and  $jj$ -coupling shell model limit ( $\Lambda = 1$ ) are known to be important for the description of the ground state. In addition to these 12 basis states, we prepare 28 basis states with various three  $\alpha$  configurations by randomly generating Gaussian center parameters. This is because, the Hoyle state is a gas-like state without specific shape, and it has been known that not only equilateral triangular configuration, various three  $\alpha$  cluster configurations couple in this state.

By superposing these 40 basis states based on GCM and diagonalizing the Hamiltonian, energy eigen states are obtained. The F1' parameter set of the Tohsaki interaction is adopted for the central part. In Fig 5, the ground  $0^+$ , first  $2^+$ , and second  $0^+$  states of  $^{12}\text{C}$  are shown together with the calculated three  $\alpha$  threshold energy (dotted line). The strength of the spin-orbit interaction,  $V_{ls}$  in Eq. 7, is chosen as  $V_{ls} = 0$  MeV,  $1600$  MeV,  $1800$  MeV, and  $2000$  MeV in (a), (b), (c), and (d), respectively. The reasonable range of the strength of  $V_{ls} = 16000 - 2000$  MeV has been suggested in the  $^4\text{He}+n$  scattering phase shift analysis [19]. Without the spin-orbit interaction ( $V_{ls} = 0$  MeV), the ground  $0^+$  state of  $^{12}\text{C}$  is obtained at  $-85.2$  MeV in Fig 5 (a) compared with the experimental value of  $-92.161726$  MeV. However, with the spin-orbit effect, the ground state is obtained at  $-87.8$  MeV in Fig 5 (b) ( $V_{ls} = 1600$  MeV),  $-88.9$  MeV in (c) ( $V_{ls} = 1800$  MeV), and  $-90.5$  MeV in

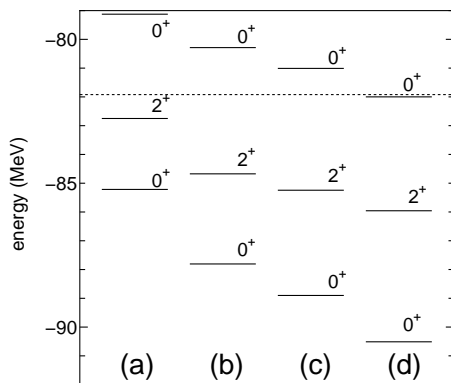


FIG. 5: The energy levels of  $^{12}\text{C}$ . Here (a) is the result without the spin-orbit interaction, and (b), (c), and (d) show the results calculated with 1600 MeV, 1800 MeV, and 2000 MeV for the strength of the spin-orbit terms of the G3RS interaction ( $V_{ls}$  in Eq. 7), respectively. The dotted line at  $-81.92$  MeV shows three  $\alpha$  threshold energy.

(d) ( $V_{ls} = 2000$  MeV). Therefore, the absolute value of the binding energy of  $^{12}\text{C}$  can be almost reproduced with the present interaction and the model, together with the binding energies of  $^4\text{He}$  and  $^{16}\text{O}$ . If we measure the energy from the three  $\alpha$  threshold energy, the ground state of  $^{12}\text{C}$  is  $-3.3$  MeV in Fig 5 (a),  $-5.9$  MeV in (b),  $-7.0$  MeV in (c), and  $-8.6$  MeV in (d), compared with the experimental value of  $-7.2747$  MeV. Thus the binding energy from the three  $\alpha$  threshold is also reproduced in the case of  $V_{ls} = 1800$  MeV (Fig 5 (c)).

The famous Hoyle state, the second  $0^+$  state experimentally observed at  $E_x = 7.65420$  MeV, appears at  $E_x = 6.1$  MeV in Fig 5 (a),  $E_x = 7.5$  MeV in (b),  $E_x = 7.9$  MeV in (c), and  $E_x = 8.6$  MeV in (d). If we measure from the three  $\alpha$  threshold energy, these energies correspond to  $E_x = 2.8$  MeV in Fig 5 (a),  $E_x = 1.6$  MeV in (b),  $E_x = 0.9$  MeV in (c), and  $E_x = -0.1$  MeV in (d). Here again  $V_{ls} = 1800$  MeV gives reasonable agreements with the experiment; however the result implies that we need slightly larger number of basis states to reproduce Hoyle state just above (experimentally 0.38 MeV) the three  $\alpha$  threshold energy.

The traditional three  $\alpha$  cluster models have a serious problem that they give very small level spacing between the ground  $0^+$  state and the first  $2^+$  state, which is the first excited state of  $^{12}\text{C}$  [1]. In our case,  $V_{ls} = 0$  MeV result in Fig 5 (a) shows that the level spacing is 2.5 MeV and much smaller compared with the experimental value of 4.4389131 MeV. This is improved by the spin-orbit effect, since the excitation from the ground  $0^+$  state to the  $2^+$  state corresponds to one-particle one-hole excitation to a spin-orbit unfavored orbit from the closure configuration of spin-orbit attractive orbits in the  $jj$ -coupling shell model. The  $0^+ - 2^+$  level spacing becomes 3.1 MeV in (b), 3.7 MeV in (c), and 4.6 MeV in (d). Similar trend has been reported in the recent antisymmetrized molecular dynamics [22] and fermionic molecular dynamics [23]

calculations.

The appearance of negative parity states in low-lying excitation energy has been considered as the signature of the importance of three  $\alpha$  cluster structure in  $^{12}\text{C}$ . Experimentally  $3^-$  and  $1^-$  states have been observed at  $E_x = 9.6415$  MeV and  $E_x = 10.84416$  MeV, respectively. These  $3^-$  and  $1^-$  states are reproduced at 9.8 MeV and 12.6 MeV, respectively, when the strength of the spin-orbit interaction is chosen as  $V_{ls} = 1800$  MeV, which gives reasonable results for the  $0^+$  and  $2^+$  states.

#### IV. SUMMARY

We have tried to achieve consistent description of  $^{12}\text{C}$  and  $^{16}\text{O}$ , which has been a long standing problem of microscopic cluster model. By taking into account the coupling with the  $jj$ -coupling shell model and utilizing Tohsaki interaction, which is finite-range three-body interaction, we have shown that consistent understanding of these nuclei can be achieved. The original Tohsaki interaction gives small overbound of about 3 MeV for  $^{16}\text{O}$ , and this is improved by slightly modifying three-body Majorana exchange parameter. Also, so far the application of Tohsaki interaction has been limited to  $4N$  nuclei, and here, we added Bartlett and Heisenberg exchange terms in the two-body interaction for the purpose of applying it to neutron-rich systems.

By applying Tohsaki interaction with finite-range three-body interaction terms to  $^{16}\text{O}$ , the lowest energy of the tetrahedron configuration of four  $\alpha$ 's is obtained with very large  $\alpha$ - $\alpha$  distance (2.5 fm). After performing GCM, the ground state is obtained with the charge radius of 2.64 fm, compared with the observed value of 2.69 fm. We often underestimate the radius by 0.1-0.2 fm with four  $\alpha$  models, if we calculate only within the two-body effective interactions, and this is significantly improved.

For  $^{12}\text{C}$ , we prepared various three  $\alpha$  configurations by randomly generating Gaussian center parameters, and we mix  $jj$ -coupling ( $\alpha$  breaking) components based on AQCM. The ground  $0^+$  state of  $^{12}\text{C}$  is obtained at  $-88.0 \sim -90.5$  MeV with reasonable strength of the spin-orbit interaction compared with the experimental value of  $-92.2$  MeV. The absolute value of the binding energy of  $^{12}\text{C}$  (and also  $^4\text{He}$  and  $^{16}\text{O}$ ) can be almost reproduced with the present interaction and the model. If we measure the energy from the three  $\alpha$  threshold energy, the agreement with the experiment is even more reasonable. The famous Hoyle state (second  $0^+$  state) is reproduced just around the three  $\alpha$  threshold energy. Also, traditional three  $\alpha$  cluster models give very small level spacing for the ground  $0^+$  state and the first  $2^+$  state, and this is significantly improved by the spin-orbit effect. The appearance of negative parity states in low-lying excitation energy has been considered as the signature of the three  $\alpha$  cluster structure of  $^{12}\text{C}$ . Experimentally  $3^-$  and  $1^-$  states have been observed at  $E_x = 9.6415$  MeV and

$E_x = 10.84416$  MeV, respectively, and these states are also reproduced within the present framework.

Yukawa Institute for Theoretical Physics, Kyoto University. This work was supported by JSPS KAKENHI Grant Numbers 716143900002.

### Acknowledgments

The author thank the discussions with Prof. A. Tohsaki. Numerical calculation has been performed at

- 
- [1] Y. Fujiwara *et al.*, Supple. of Prog. Theor. Phys. **68** 29 (1980).
- [2] F. Hoyle, D. N. F. Dunbar, W. A. Wenzel, W. Whaling, Phys. Rev. **92**, 1095c (1953).
- [3] Hisashi Horiuchi and Kiyomi Ikeda, Prog. Theor. Phys. **40**, 277 (1968).
- [4] P. Descouvemont, Phys. Rev. C **47**, 210 (1993).
- [5] Akihiro Tohsaki, Phys. Rev. C **49**, 1814 (1994).
- [6] Naoyuki Itagaki, Akira Ohnishi, and Kiyoshi Katō, Prog. Theor. Phys. **94**, 1019 (1995).
- [7] N. Itagaki, H. Masui, M. Ito, and S. Aoyama, Phys. Rev. C **71** 064307 (2005).
- [8] H. Masui and N. Itagaki, Phys. Rev. C **75** 054309 (2007).
- [9] T. Yoshida, N. Itagaki, and T. Otsuka, Phys. Rev. C **79** 034308 (2009).
- [10] N. Itagaki, J. Cseh, and M. Płoszajczak, Phys. Rev. C **83**, 014302 (2011).
- [11] T. Suhara, N. Itagaki, J. Cseh, and M. Płoszajczak, Phys. Rev. C **87**, 054334 (2013).
- [12] Tadahiro Suhara and Yoshiko Kanada-En'yo, Phys. Rev. C **91**, 024315 (2015).
- [13] N. Itagaki, H. Matsuno, and T. Suhara, Prog. Theor. Exp. Phys., in press.
- [14] A.B. Volkov, Nucl. Phys. **74**, 33 (1965).
- [15] T. Ando, K. Ikeda, and A. Tohsaki-Suzuki, Prog. Theor. Phys. **64**, 1608 (1980)
- [16] J. Decharge and D. Gogny, Phys. Rev. C **21**, 1568 (1980).
- [17] Y. Kanada-En'yo and Y. Akaishi, Phys. Rev. C **69**, 034306 (2004).
- [18] R. Tamagaki, Prog. Theor. Phys. **39**, 91 (1968).
- [19] Shigeto Okabe and Yasuhisa Abe, Prog. Theor. Phys. **61** 1049 (1979).
- [20] D.M. Brink, in *Proceedings of the International School of Physics "Enrico Fermi" Course XXXVI*, edited by C. Bloch (Academic, New York, 1966), p. 247.
- [21] I. Angeli and K. P. Marinova, At. Data Nucl. Data Tables **99**, 69 (2013).
- [22] Y. Kanada-En'yo, Phys. Rev. Lett. **81**, 5291 (1998); Y. Kanada-En'yo, Prog. Theor. Phys. **117**, 655 (2007).
- [23] T. Neff and H. Feldmeier, Nucl. Phys. **A738**, 357 (2004).